Design optimization of bendable x-ray mirrors

Wayne R. McKinney,[1*] Valeriy V. Yashchuk,[1] Kenneth A. Goldberg,[1] Malcolm Howells,[1]
Nikolay A. Artemiev,[1] Daniel J. Merthe,[1] and Sheng Yuan[2]

[1]Lawrence Berkeley National Laboratory, Berkeley, California, 94720
[2]OmniVision Technologies, 4275 Burton Drive, Santa Clara, CA, 95054 USA

ABSTRACT

Convenience and cost often lead to synchrotron beamlines where the final bendable Kirkpatrick-Baez focusing pair must relay the final image to different samples at different image distances e.g., [Proc. FEL2009, 246-249 (2009)] either for different experimental chambers, or diagnostics. We present an initial analytical approach, starting from, and extending the work of Howells et al. [OE 39(10), 2748-62 (2000)] to analyze the trade-offs between choice of mirror, bending couples and the given, shaped sagittal width of the optic. Both experimentally and in simulation, we have found that after an appropriate re-bending, sagittally shaped optics can perform with high quality at significantly different incidence angles and conjugate distances. We present one successful demonstration from the ALS Optical Metrology Beamline 5.3.1, and review some new closed form analytical solutions with a view towards understanding our results.

Keywords: bendable mirrors, x-rays, x-ray optics, optical metrology, long trace profiler, surface slope measurements, synchrotron radiation, synchrotron beamline, Kirkpatrick-Baez

1. INTRODUCTION

Due to the advantages of using optical substrates that are in hand from previous projects the staff of the current "Laboratory Directed Research and Development" (LDRD) project "X-Ray Optical Metrology for Coherence-Preserving Adaptive Optics" became interested in the use of one of these older substrates in order to save time and cost for the second, horizontal Kirkpatrick-Baez mirror in beamline 5.3.1 at the Advanced Light Source (ALS).[1-7]

We have investigated the collection of KB mirror substrates that have accumulated at the ALS optical metrology laboratory (OML) over the years, both those having sagittally straight sides and sagittally shaped sides. In a broader context, this work checks and analyzes whether previously calculated and purchased sagittally shaped substrates can be bent for different geometries of use. This could potentially involve changes in one or both of the conjugate distances, and/or the grazing incidence angle. These potential new geometries of use must be optimized and checked to see whether the required bending matches the required surface figure of the new geometry to a sufficient level for the application. The correspondence of the couples to the elastic bending of the substrate must also be checked.

2. ANALYTICAL BEGINNINGS

We begin our consideration by implementation in Mathematica™ of the formalism from Ref.[3] This will be our starting point before extending the analysis. Fig. 1 shows the optical geometry. Notation follows Ref. 3. Equation (1) shows the standard equation for a non-rotated ellipse centered on the origin. a and b are the semi-major and semi-minor axes, respectively.

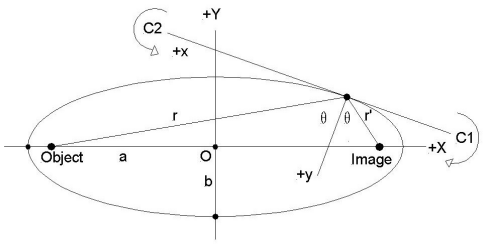

$$\frac{x^2}{a^2}+\frac{y^2}{b^2}=1 \qquad (1)$$

Figure 1: The geometry of our application of the optic bent into an off-axis ellipse. C1 is the downstream bending moment applied to the mirror. C2 is the upstream bending moment.

*wrmckinney@lbl.gov, 1-510-486-4395, fax 4385

Advances in Computational Methods for X-Ray Optics II,
edited by Manuel Sanchez del Rio, Oleg Chubar, Proc. of SPIE Vol. 8141, 81410K

The sag of the ellipse in the local coordinate system (x, y) is expanded in a MacLaurin series about the pole of the mirror,

$$y = a_2 x^2 + a_3 x^3 + a_4 x^4 + \ldots\ldots \quad . \tag{2}$$

The slope and curvature are obtained by differentiation;

$$\frac{dy}{dx} = 2a_2 x + 3a_3 x^2 + 4a_4 x^3 + \ldots\ldots \quad \text{and} \quad \frac{d^2y}{dx^2} = 2a_2 + 6a_3 x + 12a_4 x^2 + \ldots\ldots \tag{3}$$

The a_i coefficients from Ref. 3 are reproduced in Table A1, in the Appendices. We have re-derived these values.[8] The bending of the mirror is described by the Bernoulli-Euler equation,[9] where E is the elastic modulus, I(x) is the moment of inertia as a function of the tangential distance along the mirror, and C1, and C2 are the bending couples, see Fig. 1

$$E\, I(x) \frac{d^2y}{dx^2} = \frac{C1 + C2}{2} + \frac{C1 - C2}{L} x \,. \tag{4}$$

I(x) is constant for a uniform cross section, and is a function of x if the substrate is sagittally shaped. We express this as a function of the sagittal width, and, of course the thickness;

$$I(x) \;=\; \frac{b(x)\, h^3}{12} \,, \tag{5}$$

and solve for b(x), the sagittal width. h is the thickness, assumed uniform. b_0 is the thickness in the middle of the mirror, held to provide the same radius of curvature as the center of the ideal elliptical mirror,[3]

$$b(x) \;=\; \frac{b_0 \left(\frac{1}{R_0} + 6\, a_3\, x \right)}{2\, a_2 + 6\, a_3\, x + 12\, a_4\, x^2 + \ldots} \,. \tag{6}$$

We will first analyze and optimize the bending of the old substrate using the power series approach. However, our primary goal is to present our analytical solutions for the height, slope and curvature of a grazing incidence off axis ellipse expressed solely in terms of the parameters of use, and use them to find new closed form solutions for optimal sagittal shape under different assumptions. We have found analytical solutions for this width function, equation (6), see Section 5.

3. TEST CASE FOR SUBSTRATE RE-USE

For the horizontal mirror for the LDRD project we picked a suitable older substrate that had been originally purchased for mirror M3 for BL 10.3.2.[10] It is fabricated from single crystal silicon, 102 mm long, 13 mm in sagittal width in the middle, and 4 mm thick. See Table 1, for its parameters of use, and for the parameters of the new intended use at BL 5.3.1. For the new use, r comes in from infinity, r' is a little shorter, and the grazing incidence angle is doubled. We now wish to bend the substrate to an ellipse, rather than a parabola.

Table 1: Geometry of use for the mirror substrate: new, and old.

	source to mirror distance	mirror to image distance	incidence angle from normal
Old use: M3, BL 10.3.2	$r = \infty$	r' = 260 mm	$\theta = \pi/2 - 0.004$
New Use: Horizontal Mirror, BL 5.3.1	r = 1525.76 mm	r' = 243.63 mm	$\theta = \pi/2 - 0.008$

Fig. 2a shows the optimal radius of curvature needed for the before and after uses. Fig. 2b shows the optimal sagittal width of the substrate in question from the old use, and sagittal width given by the old formalism for the new usage. Note that they are quite different.

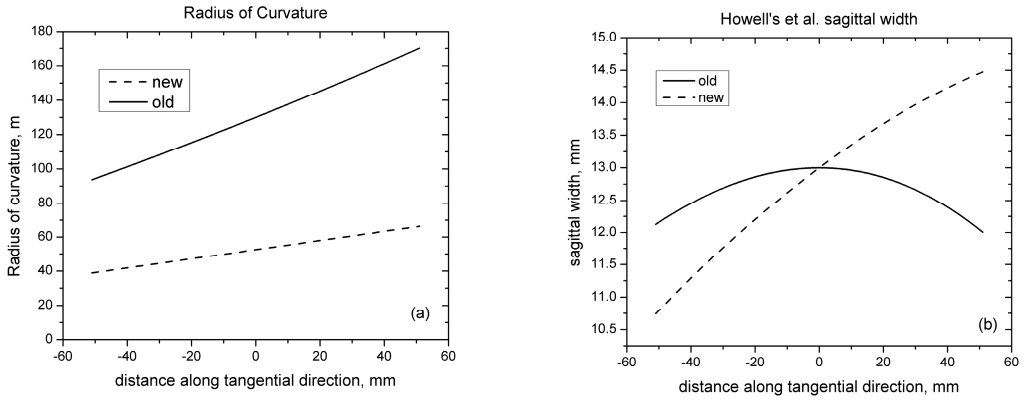

Figure 2: (a) radii of curvature for the before and after uses. (b) optimal sagittal width according to Eq. (6) for each use. Downstream is on the left in each graph, see notation in Fig. 1. Of course, since we are using an old substrate, and not buying a new one, we only have access to a mirror with the sagittal shape on the right plotted by the solid line.

The solution of the bending equation given in Ref. [3] including Eq. (6) assumes that the couples C1 and C2 are those computed by maintaining the condition that the width of the mirror in the center is held constant. Stated another way, the this means that the radius of curvature in the center of the mirror be the same as that of the exact ellipse, in each different case. This constant width at x = 0 is shown by the crossing at the center point of the two curves in Fig. 2b. For the existing sagittal width (solid line in the figure) the left hand side (downstream) value of 12.126 mm is larger than the 12.000 mm right hand side (upstream) value. This is a result of optimization with the used boundary conditions. The couples under this assumption are (0.0897 Nm, 0.0489 Nm) for the original case, and (0.2169 Nm, 0.1263 Nm) for the new case. Bending couples that are this different make bending and tuning more difficult. The bender, finding a new equilibrium position in translation as it is tightened, can move along the beamline. To address this problem the two leaf springs are often made of different thicknesses, causing yet another set of differences, and hence problems, in the mechanism.

It is straightforward in Mathematica™ to numerically integrate the second order differential Eq. (4) to obtain the height and slope predicted by the bending. We should have some indication of the accuracy of the calculation, however, before making conclusions at nanometer, and sub-microradian levels. Figure 3 shows the height and slope obtained from the integration for the old case, solid lines; and the new case, dotted lines. The width function was interpolated by cubic spline between points 1 mm apart for the integration. Two necessary and sufficient boundary conditions are supplied by setting the height and slope to zero at the center of the optic. We find that the height differs less than 10^{-8} mm from the exact elliptical cylinder, and the slope differs by less than 10^{-9} radian for both cases, showing the accuracy of our numerical implementation of Eq. (4) in Mathematica.™ Our considerations do not include gravity, chamfers, edge rounding, and anticlastic bending; some or all of which might have to be considered when designing a larger or differently shaped mirror.

4. PERFORMANCE AT THE NEW USE PARAMETERS

We now look at the difference in the new case between the shape achieved by bending and the exact elliptical cylinder. We find in Fig. 4, when re-integrating the differential Eq.(4) for the new case, the somewhat surprising result that the mirror performs quite well in the new geometry, even at twice the bending (solid lines) of the original design. The rms deviation in slope is 0.49 μrad for the entire length, and just 0.23 μrad over the central 80 mm clear aperture. Thus, the substrate can perform near the diffraction limit for our new application, even without relaxing the criterion of matching the radius of the new ellipse in the middle.

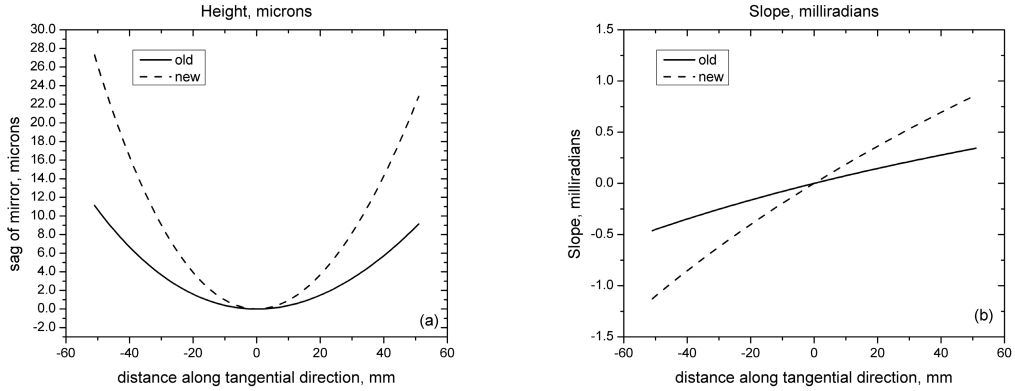

Figure 3: Height and slope predictions from numerical integration of the Bernoulli-Euler differential equation: (a) height or sag of the mirror; (b) slope of the mirror. Downstream is on the left. Solid lines are the substrate in the original use, dashed lines are the substrate bent to the new use, maintaining the condition that the radius of the ellipse at the pole of the mirror be the same as that of the exact elliptical cylinder for that case.

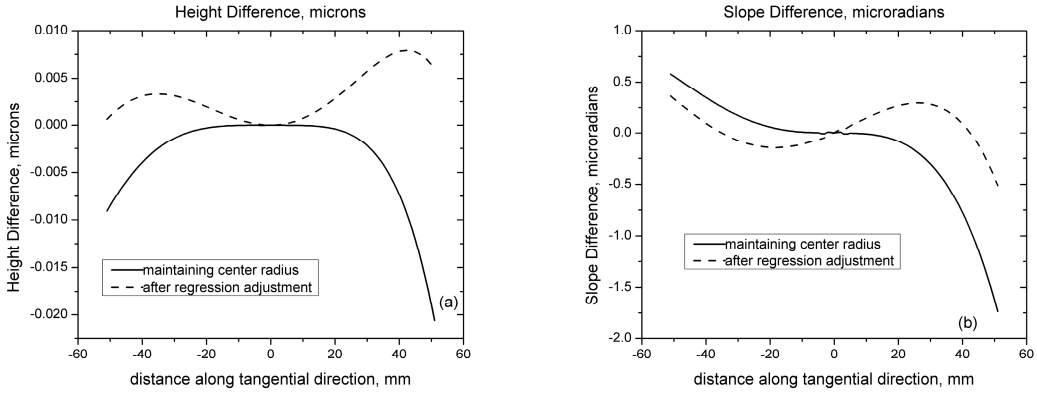

Figure 4: Height and slope differences from exact elliptical figure. (a) height difference in microns. (b) slope difference in microradians. Downstream is on the left. Solid lines, maintaining center radius; dashed lines, after regression adjustment of couples, allowing a different center radius.

We are clearly not at optimal adjustment, however. The height difference in Fig. 4a (solid line) does not show the characteristic "bird" to be expected from optimal balancing of second and fourth order aberrations,[11] and the slope in Fig. 4b (solid line) shows a net tilt. We now execute an optimization in exact analogy to the adjustment procedures done on mirrors sent for adjustment in the OML.[12,13] We tune the couples one at a time a known small amount. In this case we stepped C1 and then C2 by 1% of the sum of the two original couples. This gives us the effect of a small adjustment in each couple. Given enough independence between the effects on the mirror of each couple, we can then solve for optimal changes in C1 and C2 which serve to optimize the difference between the as bent surface and the ideal tangential elliptical figure.

Recalling the development from Refs [11,12], we re-write equation (4), putting all effects except the effects of the couples into two new functions;

$$\frac{d^2y}{dx^2} = C_1 g_1(x) + C_2 g_2(x)\,, \qquad (7)$$

where we have defined:

$$g_1(x) = \left(\frac{1}{2} - \frac{1}{L}x\right)\frac{1}{EI(x)} \text{ and } g_2(x) = \left(\frac{1}{2} + \frac{1}{L}x\right)\frac{1}{EI(x)}. \quad (8)$$

Integrating (7) provides the slope,

$$\alpha(x,C) \equiv \frac{dy}{dx} = C_0 + C_1\, f_1(x) + C_2\, f_2(x), \quad (9)$$

where

$$f_1(x) = \int g_1(x)\,dx \quad \text{and} \quad f_2(x) = \int g_2(x)\,dx. \quad (10)$$

C_0 is a constant of integration that is the overall tilt of the mirror. We have expressed the slope trace of a bendable mirror as a linear combination of two functions, $f_1(x)$ and $f_2(x)$, specific to the mirror design. We now consider f_1 and f_2 to be unknown functions which we will determined by approximation later, and identify the components of the vector C to be the adjustments of the bendable mirror in whatever units are convenient. The errors in the surface slope with respect to the ideal elliptical surface are linear in these not yet determined functions. If these functions were known, one would directly optimize the mirror shape to the desired one by varying the constants C_1 and C_2. Consider an ideal elliptical surface in the same notation:

$$\alpha^0(x,C) = C_0^0 + C_1^0\, f_1(x) + C_2^0\, f_2(x). \quad (11)$$

Deviations from the ideal surface slope may be expressed:

$$\Delta\alpha(x,C) = \Delta C_0 + \Delta C_1\, f_1(x) + \Delta C_2\, f_2(x). \quad (12)$$

We now proceed to approximate the values of the $f_i(x_i)$. If we calculate the slope of the optic for any given set of adjustments of the C_i:

$$\delta\alpha_{20}(x_i) = \Delta C_0 + \Delta C_1\, f_1(x_i) + \Delta C_2\, f_2(x_i), \quad (13)$$

and then adjust one of the couples, say the left bending moment, represented by C_1 and calculate the mirror again at the new setting :

$$\delta\alpha_{21}(x_i) = \Delta C_0 + (\Delta C_1 + \delta C_1) f_1(x_i) + \Delta C_2\, f_2(x_i), \quad (14)$$

we may subtract (13) from (14) resulting in:

$$\delta\alpha_{21}(x_i) - \delta\alpha_{20}(x_i) = \delta C_1\, f_1(x_i) \quad (15)$$

We may solve for an approximation to f_1,

$$f_1^*(x_i) = \frac{\delta\alpha_{21}(x_i) - \delta\alpha_{20}(x_i)}{\delta C_1}. \quad (16)$$

With the asterisk we separate the estimate from the true value of the function. Analogously, we may repeat the process by differencing two calculations of the slope of the optic with different values of the other couple.

$$f_2^*(x_i) = \frac{\delta\alpha_{22}(x_i) - \delta\alpha_{20}(x_i)}{\delta C_2} \quad (17)$$

Now using the $f_i^*(x_i)$, linear regression analysis can be applied to find the best fit adjustment parameters.[14-18] First the regression matrix may be formulated:

$$\hat{A} \approx \begin{bmatrix} 1 & f_1^*(x_1) & f_2^*(x_1) \\ 1 & f_1^*(x_2) & f_2^*(x_2) \\ \vdots & \vdots & \vdots \\ 1 & f_1^*(x_m) & f_2^*(x_m) \end{bmatrix}. \quad (18)$$

This provides a solution:[16]

$$\Delta\hat{C}^* = (\hat{A}'\hat{A})^{-1}\hat{A}'\delta\alpha_{20}, \quad (19)$$

with an estimation for the dispersion of the found parameters:

$$D(\Delta\hat{C}^*) = \sigma^2(\hat{A}'\hat{A})^{-1}, \quad (20)$$

where the dispersion parameter σ^2 can be estimated from:

$$\sigma^2 \approx \frac{\sum_i [\delta\alpha_{20} - \Delta C_1^* f_1^*(x_i) - \Delta C_2^* f_2^*(x_i)]^2}{m-p}. \quad (21)$$

Where p is the number of parameters plus 1. (In our mirror bending applications p = 4.)

In this new calculational, rather than experimental, application we implement the 3 sets of couples by three integrations of Eq. (4) rather than in three adjustments of an actual mirror. Assuming linearity of the problem, we predict by the method summarized in Eqs. [(7)-(21)] a new (C1,C2) pair using characteristic functions computed by differences in the 3 results divided by the step amounts in the couples.[13] Fig. 5 shows the three slope trace differences of our method from the exact elliptical shape. It is exactly analogous to computing a change table in geometrical optics, and predicting a best solution from the

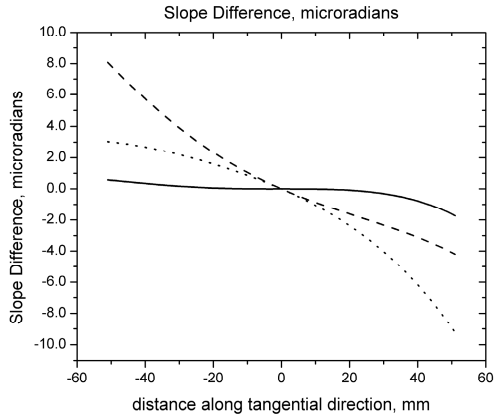

Figure 5 Slope differences between the three different mirror shapes used to predict optimal adjustment by regression analysis, and the exact elliptical shape. Solid line repeats the slope differences from the right hand side of Fig. 4. Dotted and dashed traces are the slope differences when C1 and then C2 are stepped a small amount according to the method.

shifts in a merit function that occur as a result of the changes.[19] The new couples change only slightly to achieve this adjustment. Even though the change is small, the effect on the result is significant. The newly predicted performance is shown by the dashed lines in Fig. 4. Notice the much better "bird" shown in Fig. 4a (dashed line), and the now near zero tilt of the slope in Fig. 4b. While "bird" is not an end in itself--lower rms error is--it does indicate that we have exhausted all the possible adjustments available with two couples, and balanced 2nd and 4th order aberrations.[11] It also indicates that 3rd order aberration (coma) has been adjusted out. The new couples give rms slopes of 0.19 μrad rms full length, and 0.17 μrad rms over an 80 mm clear aperture (dashed lines in Figs. 4a and 4b). When bendable optics are adjusted in the OML this balance of second and fourth order aberrations is now routine as a sign that the maximum reduction of the rms deviation from exact tangentially elliptical figure is close.

We have shown that an old substrate from BL 10.3.2 can be used for the LDRD project on BL 5.3.1 despite the different parameters of use for which it was sagittally shaped in manufacture. The vertically deflecting KB mirror with the considered substrate has been assembled and successfully adjusted at the OML to the new calculated parameters. We next turn to why this can be so by looking at the finer details of sagittal shaping.

5. ANALYTICAL RESULTS

It is the conditions under which these results were derived that we wish to modify slightly. Ref. [3] fixes the curvature in the center of the mirror to that given by the focusing term (Coddington's tangential equation). The authors then match the first two or three terms in the equation for the curvature [times E I(x)] with the right hand side of Eq. (5), and solve for the two couples C1, and C2. Keeping these couples, they then solve for the sagittal width with a very precise 10^{th} order polynomial expansion of the exact tangentially elliptical shape, see Appendix A.

We now restart the derivation, still within the power series formalism; and, as does Ref [3], we vary the number of terms used to find the couples C1, and C2. In Mathematica,™ we break out the three terms of defocus, coma, and spherical aberration:

$$\text{defocus} = 2\,E\,I(x)\,a_{02} \qquad \text{coma} = 6\,E\,I(x)\,a_{03}\,x \qquad \text{sphaber} = 12\,E\,I(x)\,a_{04}\,x^2 \quad . \tag{22}$$

b appears implicitly in Eq. (22) implicitly through Eq. (5). Next we solve Eq. (4) for the sagittal width: (shown in Mathematica™ syntax);

$$\text{Solve}\left[\left\{\text{defocus}+\text{coma}+\text{sphaber}==(C1+C2)/2+(C1-C2)*x/L\right\},\{b\}\right] . \tag{23}$$

Our analytical result is, where we have added 234 as subscripts to b, the width, to indicate the orders of the 3 aberrations:

$$b_{234}(x)=\frac{96\,r^3r'^3\,(C1\,L+C2\,L+2C1\,x-2\,C2\,x)\,\text{Sec}[\theta]}{E\,h^3L(r+r')\begin{pmatrix}8\,r^2r'^2+12\,r\,r'x^2-12\,r^2r'x\,\text{Sin}[\theta]+12\,r\,r'^2x\,\text{Sin}[\theta]+15\,r^2x^2\,\text{Sin}^2[\theta]\\-30\,r\,r'x^2\text{Sin}^2[\theta]+15\,r'^2x^2\,\text{Sin}^2[\theta]\end{pmatrix}} . \tag{24}$$

We now modify this result by leaving out the spherical aberration term in order to show that a straight-sided substrate can eliminate both defocus and coma for a selected pair of C1, and C2; (This result is seen to be trivial by comparing terms of similar order in x on both sides of the equation.)

$$\text{Solve}\left[\left\{\text{defocus+coma}==(C1+C2)/2+(C1-C2)\;x/L\right\},\{b\}\right] . \tag{25}$$

This gives the following result for $b_{23}(x)$, where the subscripts, again, indicate the terms included in the derivation,

$$b_{23}(x) \;=\; \frac{24\,r^2r'^2\,(C1\,L+C2\,L+C1\,x-2\,C2\,x)\,\text{Sec}[\theta]}{E\,h^3\,L\,(r+r')\,(2\,r\,r'-3\,r\,x\,\text{Sin}[\theta]+3\,r'x\,\text{Sin}[\theta])} \tag{26}$$

To find our next desired result, Eq. (28) , we have differentiated Eq. (26) with respect to x, and set the result equal to zero finding the (C1,C2) pair ratio which allows for a constant sagittal width, Eq. (27).

$$C2_{23} \;=\; -C1_{23}\,\frac{(-4r\,r'-3\,L\,r\,\text{Sin}[\theta]+3\,L\,r'\,\text{Sin}[\theta])}{(4\,r\,r'-3\,L\,r\,\text{Sin}[\theta]+3\,L\,r'\,\text{Sin}[\theta])} \tag{27}$$

Substituting (27) back into (26) we find;

$$b_{23} = \text{const.} = \frac{96\ C1\ r^2 r'^2 \text{Sec}[\theta]}{E\ h^3 \left(r + r'\right)\left(4\ r\ r' + 3\ L\left(-r + r'\right)\text{Sin}[\theta]\right)} \tag{28}$$

Note that there is no dependence on x in Eq. (28). We now have the satisfying result that explains why significant performance may be sometimes achieved with a less than optimal shape—the two biggest aberrations, defocus and coma, may be corrected with a sagittally un-shaped substrate.

To recap, we have shown explicitly that to third order, accounting defocus and coma, a straight sided bender can give optimal performance if the sagittal width is chosen by expression (26), and the C2/C1 ratio is chosen by expression (27) Moreover, we have shown that to fourth order there is a closed form solution to the sagittal width.

Indeed, the similarity of the numerators between expression (24), and expression (26) suggests that the 3 aberration case might be approached in a similar manner:

$$C2_{234} = \frac{C1_{234}\left(4\ r\ r'\left(2\ r\ r' - 3\ x\left(L + x\right)\right) + 3\left(-r + r'\right)\text{Sin}[\theta]\left(-2\ L\ r\ r' + 5\left(r - r'\right)x\left(L + x\right)\text{Sin}[\theta]\right)\right)}{\left(4\ r\ r'\left(2\ r\ r' + 3\ x\left(L - x\right)\right) + 3\left(-r + r'\right)\text{Sin}[\theta]\left(2\ L r\ r' + 5\left(-r + r'\right)x\left(L - x\right)\text{Sin}[\theta]\right)\right)}. \tag{29}$$

Unfortunately, the x dependence remains, and we find no neat solution for a substrate of constant sagittal width to fourth order. However, we did achieve balancing between second and fourth orders in our results in sections 3, and 4 with a wrongly shaped substrate. Even for a straight sided bender, balancing these orders will provide performance exceeding that given by our analytical results in this section.[11]

6. EXACT EXPRESSION FOR THE ELLIPTICAL FIGURE

We now break completely with the series expansion formalism. If we return to Eq. (4), and replace the three pieces of the curvature linked to the three aberrations with the analytical closed form of the curvature for an exact off-axis ellipse, we can solve analytically for a closed form solution for the sagittal width.

We use for the total curvature of a grazing incidence off-axis ellipse: (see Appendix B)

$$\text{curv}_{\text{tot}} = \frac{r^2 r'^2 \left(r + r'\right)^4 \left(1 + \text{Cos}[2\theta]\right)^2}{8\left(-r\ r'\left(r + r'\right)^2 \text{Cos}^2[\theta]\left(-r\ r' + x^2 + \left(r - r'\right)x\ \text{Sin}[\theta]\right)\right)^{\frac{3}{2}}}. \tag{30}$$

This closed form expression for the curvature, (30), may be checked against Ref. [3] by taking a MacLaurin expansion to second order;

$$\text{curv}_{\text{tot}} = \frac{\left(r + r'\right)\text{Cos}[\theta]}{2\ r\ r'} + \frac{3}{8\left(\frac{-1}{r^2} + \frac{1}{r'^2}\right)\text{Sin}[2\theta]\,x} + \frac{3\left(r + r'\right)\text{Cos}[\theta]\left(5r^2 - 2r\ r' + 5r'^2 - 5\left(r - r'\right)^2 \text{Cos}[2\theta]\right)x^2}{32 r^3\ r'^3} + \ldots\ldots. \tag{31}$$

Comparison shows that after multiplying each term by E b(x) $h^3/12$ that the terms match those of Ref. [3], confirming our result from Appendix B.

Putting expression (30) into (4), or practically into (23), and solving, we have;

$$b_{tot,ellipsoid}(x) = \frac{96\left(\frac{C1+C2}{2}+\frac{C1-C2}{L}\right)\left(-r\,r'\left(r+r'\right)^2\,Cos^2\left[\theta\right]\left(-r\,r'+x^2+\left(r-r'\right)x\,Sin\left[\theta\right]\right)\right)^{\frac{3}{2}}}{E\,h^3\,r^2\,r'^2\left(r+r'\right)^4\left(1+Cos\left[2\theta\right]\right)^2}\,. \qquad (32)$$

This provides our nearly penultimate result: the sagittal width function for an off-axis elliptically cylindrically bent optic as a function of the parameters of the geometry of use, and the two bending couples. Finally, we take the limiting case of a cylindrically paraboloidal bent optic, and insert (B9) into (4), finding;

$$b_{tot,paraboloid} = \frac{3\,(C1\,L+C2\,L+2\,C1\,x-2\,C2\,x)(r'-x\,Sin[\theta])^2}{16\,E\,L\sqrt{r'\,Cos[\theta]^2\,(r'-x\,Sin[\theta])}} \qquad (33)$$

7. CONCLUSIONS

We have found that previously purchased substrates for tangentially elliptical bendable optics should be checked to see if they can be used in other geometries. Specifically, we showed that a substrate originally shaped to become a parabola for beamline 10.3.2 can readily be adapted to an elliptical shape for nano-focusing and wavefront optimization research on ALS beamline 5.3.1. In order to explain this we have clarified previous work by expressing the optimal form of sagittal shaping for bendable mirrors in closed form solutions for the two cases of defocus plus coma, and defocus plus coma plus spherical aberration using the previous polynomial expression for the elliptical shape. The benefits of this theory--allowing the slope at the mirror center to find an optimal value not fixed to a prescribed slope--are that the mathematical formulation now matches alignment shapes attained when bending mirrors experimentally.

Continuing, we inserted an exact expression for the curvature of an off-axis ellipse, and found a useful closed form expression for the optimal sagittal width for the completely exactly formulated case, both for the ellipsoidal and paraboloidal cases. Taken together, these results illustrate more completely what is actually done when optimizing the adjustment of a bendable optic in the laboratory, or beamline.

APPENDIX A

Table A1: MacLaurin expansion coefficients of a tangential elliptical cylinder, after Ref.[8] u and v are defined for convenience. r, r' and θ are positive definite, θ being measured from the normal. Since de-magnifications can now exceed 100 to 1 this many terms are necessary when using the series approximation to the tangential elliptical figure. These expressions have been confirmed as part of this work.

$u \equiv Sin[\theta]\left(\frac{1}{r}-\frac{1}{r'}\right)$	$v \equiv \frac{1}{r\,r'}$
$a_0 = 0$ (origin is at the pole of the optic)	$a_1 = 0$ (slope is zero at the pole of the optic)
$a_2 = \frac{\cos[\theta]}{4}\left(\frac{1}{r}+\frac{1}{r'}\right)$	$a_3 = \frac{a_2\,u}{2}$
$a_4 = a_2\left(\frac{5u^2}{16}+\frac{v}{4}\right)$	$a_5 = a_3\left(\frac{7u^2}{16}+\frac{3v}{4}\right)$
$a_6 = a_2\left(\frac{21u^4}{128}+\frac{7u^2\,v}{16}+\frac{v^2}{8}\right)$	$a_7 = a_3\left(\frac{33u^4}{128}+\frac{15u^2\,v}{16}+\frac{5v^2}{8}\right)$
$a_8 = a_2\left(\frac{429u^6}{4096}+\frac{495u^4\,v}{1024}+\frac{135u^2\,v^2}{256}+\frac{5v^2}{64}\right)$	$a_9 = a_3\left(\frac{715u^6}{4096}+\frac{1001u^4\,v}{1024}+\frac{385u^2\,v^2}{256}+\frac{35v^2}{64}\right)$
$a_{10} = a_2\left(\frac{2431u^8}{32768}+\frac{1001u^6\,v}{2048}+\frac{1001u^4\,v^2}{1024}+\frac{77u^2\,v^2}{128}+\frac{35v^4}{128}\right)$	

APPENDIX B

Our goal is to provide, in closed form, the equation of the surface, its derivative the slope, and its second derivative which is equal to the curvature in our approximation with only r, r', and θ as independent variables.

We begin with Eq. (1) and a slightly different accompanying diagram, Fig. B1, where we have moved the ellipse to satisfy the extreme off-axis nature of grazing incidence;

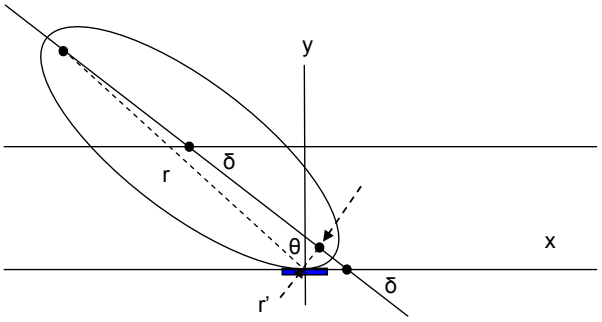

Figure B1: Translated and rotated ellipse

$$\frac{x^2}{a^2}+\frac{y^2}{b^2}=1\,. \tag{A1}$$

We require our equations change to have their origin of coordinates at the center of the optic with the normal to the surface at this point the y-axis. To achieve this, we must translate the ellipse and rotate it. We rotate the ellipse first.

$$\frac{\left(x\mathrm{Cos}[\delta]+y\mathrm{Sin}[\delta]\right)^2}{a^2}+\frac{\left(x\mathrm{Sin}[\delta]-y\mathrm{Cos}[\delta]\right)^2}{b^2}=1\quad . \tag{A2}$$

Equation (A2) obtains because we are rotating by -δ. That is, since counter clockwise is by convention defined as positive, our clockwise rotation requires a negative angle in the standard notation. The rotation matrix equation for points with -δ inserted is;

$$\begin{pmatrix} x_{rot} \\ y_{rot} \end{pmatrix}=\begin{pmatrix} \mathrm{Cos}[-\delta] & -\mathrm{Sin}[-\delta] \\ \mathrm{Sin}[-\delta] & \mathrm{Cos}[-\delta] \end{pmatrix}\begin{pmatrix} x \\ y \end{pmatrix}\quad . \tag{A3}$$

Note that this is the transpose of the standard matrix which rotates coordinate systems. Multiplying out, we obtain;

$$x_{rot}=x\mathrm{Cos}[\delta]+y\mathrm{Sin}[\delta]\quad y_{rot}=-x\mathrm{Sin}[\delta]+y\mathrm{Cos}[\delta]\ , \tag{A4}$$

which is what we have used for (A2). Note that δ is now positive definite because we have explicitly accounted the signs. Because of the squares in (A2), y_{rot} can be reversed in sign for better symmetry without affecting further results. If we multiply out (A2), and collect terms according to the most general equation for an ellipse:[20]

$$A\left(x-x_c\right)^2+B\left(y-y_c\right)^2+C\left(x-x_c\right)+D\left(y-y_c\right)+E\left(x-x_c\right)\left(y-y_c\right)+F=0\ , \tag{A5}$$

we find these results. Note that (A5) includes a translation of the center of the ellipse to the coordinates (x_c,y_c).

$$
\begin{aligned}
A &= b^2\mathrm{Cos}^2[\delta] + a^2\mathrm{Sin}^2[\delta],\\
B &= a^2\mathrm{Cos}^2[\delta] + b^2\mathrm{Sin}^2[\delta],\\
C &= -2x_c\left(b^2\mathrm{Cos}^2[\delta] + a^2\mathrm{Sin}^2[\delta]\right) + (a-b)(a+b)\,y_c\mathrm{Sin}[2\delta],\\
D &= -2y_c\left(a^2\mathrm{Cos}^2[\delta] + b^2\mathrm{Sin}^2[\delta]\right) + (a-b)(a+b)\,x_c\mathrm{Sin}[2\delta],\\
E &= \left(-a^2 + b^2\right)\mathrm{Sin}[2\delta],\\
F &= -a^2b^2 + \left(b^2x_c^{\,2} + a^2y_c^{\,2}\right)\mathrm{Cos}^2[\delta] + \left(a^2x_c^{\,2} + b^2y_c^{\,2}\right)\mathrm{Sin}^2[\delta] + \left(-a^2 + b^2\right)x_cy_c\mathrm{Sin}[2\delta].
\end{aligned}
\tag{A6}
$$

Since we have two boundary conditions in the final translated coordinate system: from y = y' = 0 at x = 0, we can show that C = F = 0 must hold for our final results, see (A7) and (A8). Note that we are not using (x_c,y_c) for these conditions because we have translated to the new coordinates, and (x_c,y_c) are now the coordinates of the center of the ellipse.

$$
\begin{aligned}
&y = 0 \quad \text{at} \quad x = 0 \quad \Rightarrow\\
&A\,x^2 + B\,y^2 + C\,x + D\,y + E\,x\,y + F = 0,\\
&0 + 0 + 0 + 0 + 0 + F \;=\; 0 \quad \Rightarrow \quad F = 0 \quad .
\end{aligned}
\tag{A7}
$$

$$
\begin{aligned}
&y = y' = 0 \quad \text{at} \quad x = 0 \quad \Rightarrow\\
&\frac{d}{dx}\left(A\,x^2 + B\,y^2 + C\,x + D\,y + E\,x\,y + F\right) = 0,\\
&2\,A\,x + 2\,B\,y\,y' + C + D\,y' + E\,y + E\,x\,y' + 0 = 0,\\
&0 + 0 + C + 0 + 0 + 0 + 0 = 0 \qquad \Rightarrow \quad C = 0.
\end{aligned}
\tag{A8}
$$

APPENDIX C

To completely remove all of our parameters from those of the non-translated, non-rotated ellipse we now find a, b, δ, x_c, and y_c directly from the optical parameters r, r', and θ, where θ is the angle of incidence at the center of the mirror measured from the normal. θ is the angle of incidence measured from the normal, and is positive definite.

$2a = r + r'$ is straightforward, finding the semi-major axis, a, using only optical parameters. Drawing the special case when the pole of the mirror is at the top center of the ellipse drawn in Fig. C1, we have, then;

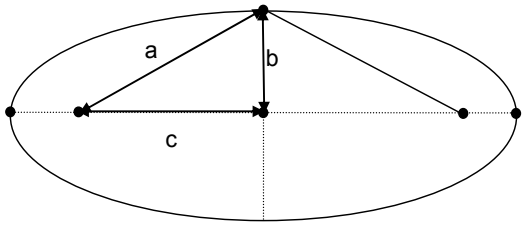

Figure C1: Geometry of the ellipse for finding b

$$
\begin{aligned}
&b^2 = a^2 - c^2 = \left(\frac{r + r'}{2}\right)^2 - c^2 = \frac{\left(r + r'\right)^2}{4} - c^2 \quad 4b^2 = \left(r + r'\right)^2 - 4c^2\\
&\left(2b\right)^2 = \left(r + r'\right)^2 - \left(2c\right)^2 \qquad b = \frac{1}{2}\sqrt{\left(r + r'\right)^2 - \left(2c\right)^2}\,.
\end{aligned}
\tag{B1}
$$

$\left(2c\right)^2$ may now be found with the cosine rule, giving the semi-minor axis in terms of the optical parameters;

$$
\left(2c\right)^2 = r^2 + r'^2 - 2\,r\,r'\mathrm{Cos}[2\theta].
\tag{B2}
$$

$$b = \frac{1}{2}\sqrt{(r+r')^2 - (2c)^2} = \frac{1}{2}\sqrt{(r+r')^2 - (r^2 + r'^2 - 2\,r\,r'\,\mathrm{Cos}[2\theta])}$$

$$\frac{1}{2}\sqrt{r^2 + r'^2 + 2\,r\,r' - r^2 - r'^2 + 2\,r\,r'\,\mathrm{Cos}[2\theta]} = \frac{1}{2}\sqrt{2\,r\,r' + 2\,r\,r'\,\mathrm{Cos}[2\theta]} \tag{B3}$$

$$b = \frac{1}{2}\sqrt{2\,r\,r'(1+\mathrm{Cos}[2\theta])}$$

In order to obtain and x_c and y_c directly from the optical parameters we examine the center of the ellipse in Fig. B1;

$$[x_c, y_c] = \left[\frac{(-r\,\mathrm{Sin}[\theta] + r'\,\mathrm{Sin}[\theta])}{2},\ \frac{(r\,\mathrm{Cos}[\theta] + r'\,\mathrm{Cos}[\theta])}{2}\right] \tag{B4}$$

δ is found by computing the slope of the line through the two foci in Fig. B1, using the two focal points, and taking the inverse tangent of the slope, m, to get the angle;

$$\delta = \mathrm{Tan}^{-1}[m] = \mathrm{Tan}^{-1}\left[\frac{r\,\mathrm{Cos}[\theta] - r'\,\mathrm{Cos}[\theta]}{-r\,\mathrm{Sin}[\theta] - r'\,\mathrm{Sin}[\theta]}\right] =$$

$$\mathrm{Tan}^{-1}\left[\frac{(r-r')}{(-r-r')}\frac{\mathrm{Cos}[\theta]}{\mathrm{Sin}[\theta]}\right] = \mathrm{Tan}^{-1}\left[-\frac{(r-r')}{(r+r')}\mathrm{Cot}[\theta]\right]. \tag{B5}$$

We now have δ as a trigonometric function of a ratio of functions of our three optical parameters. Returning to our results for the equation of the rotated and translated ellipse, Eqs. (A6), we can express the height, of the exact translated, rotated, tangentially elliptical surface:

$$\mathrm{height} = -(r+r')\left(-4r\,r'\mathrm{Cos}[\theta] + 4\mathrm{Abs}[\mathrm{Cos}[\theta]]\sqrt{r\,r'(r\,r' - x^2 + (-r+r')\,x\,\mathrm{Sin}[\theta])} + (r-r')\mathrm{Sin}[2\theta]\right) \Big/ \left(r^2 + 6r\,r' + r'^2 - (r-r')^2\,\mathrm{Cos}[2\theta]\right). \tag{B6}$$

A similar expression to (B6) is found in Ref.[21] on crystal spectrometers which differs from this because it uses the grazing incidence angle, the complement of our angle from the normal, and it has another method of derivation. Numerically both Ref. [21] Eq. (15) and our Eq. (B6) give the same result. Slope and curvature are readily obtained by differentiation, although getting them into compact forms requires some manipulation in Mathematica.™ Rommeveaux et al.[22] give results for the height and slope of the off-axis ellipse, and Zhang et al.[23] solve the same Bernoulli-Euler equation, but do not explicitly present the formulas for the off-axis ellipse. To our knowledge, this is the first complete collection of the expressions, using only the conjugate distances, and the normal incidence angle.

$$\mathrm{slope} = 2\,r\,r'(r+r')\mathrm{Cos}^2[\theta](2x + (r-r')\mathrm{Sin}[\theta]) - \mathrm{Abs}[\mathrm{Cos}[\theta]](r^2 + r'^2 - 2r\,r'\mathrm{Cos}[2\theta])\sqrt{r\,r'(r\,r' - x^2 + (-r+r')\,x\,\mathrm{Sin}[\theta])}\ \mathrm{Sin}\left[2\,\mathrm{Tan}^{-1}\left[\frac{(r-r')\mathrm{Cot}[\theta]}{r+r'}\right]\right] \Big/ \mathrm{Abs}[\mathrm{Cos}[\theta]]\left(r^2 + 4r\,r' + r'^2 + 2r\,r'\mathrm{Cos}[2\theta] + (r^2 + r'^2 - 2r\,r'\mathrm{Cos}[2\theta])\mathrm{Cos}\left[2\,\mathrm{Tan}^{-1}\left[\frac{(r-r')\mathrm{Cot}[\theta]}{r+r'}\right]\right]\right)\sqrt{r\,r'(r\,r' - x^2 + (-r+r')\,x\,\mathrm{Sin}[\theta])} \tag{B7}$$

$$\mathrm{curvature} = \frac{r^2\,r'^2\,(r+r')^4\,(1+\mathrm{Cos}[2\theta])^2}{8\left(-r\,r'(r+r')^2\,\mathrm{Cos}^2[\theta](-r\,r' + x^2 + (r-r')\,x\,\mathrm{Sin}[\theta])\right)^{\frac{3}{2}}} \tag{B8}$$

These three results may be straightforwardly applied to the case of a paraboloidal optic by taking the limit as r goes to infinity:

$$\text{paraboloid's curvature} = \frac{\sqrt{r' \text{Cos}[\theta]^2 (r' - x \text{Sin}[\theta])}}{2(r' - x \text{Sin}[\theta])^2}, \tag{B9}$$

the slope of the paraboloid;

$$\text{Cot}[\theta] \left(-1 + \frac{r' \text{Cos}[\theta]}{\text{Abs}[\text{Cos}[\theta]] \sqrt{r' (r' - x \text{Sin}[\theta])}}\right), \tag{B10}$$

and the height, or sag of the paraboloid;

$$-\text{Cot}[\theta] (x - 2 r' \text{Csc}[\theta]) - 2 \text{Abs}[\text{Cos}[\theta]] \text{Csc}[\theta]^2 \sqrt{r' (r' - x \text{Sin}[\theta])}. \tag{B11}$$

ACKNOWLEDGEMENTS

The authors wish to thank Ken Chow of the Lawrence Berkeley National Laboratory Engineering Division for discussions and comparison of numerical results, and all the members of the Beamline 5.3.1 LDRD team.

The Advanced Light Source is supported by the Director, Office of Science, Office of Basic Energy Sciences, Material Science Division, of the U.S. Department of Energy and by the DOE Laboratory Directed Research and Development Program under Contract No. DE-AC02-05CH11231 at Lawrence Berkeley National Laboratory.

REFERENCES

[1] Kelez, N., Bozek, J., Chuang, Y.-D., Duarte, R., Lee, D. E., McKinney, W., Yashchuk, V. *et al.*, "Design, Modeling, and Optimization of Precision Bent Refocus Optics - LCLS AMO KB Mirror Assembly," FEL2009, 546-549 (2009).

[2] Kelez, N., Chuang, Y.-D., Smith-Baumann, A., Franck, K., Duarte, R., Lanzara, A., Hasan, M. Z. *et al.*, "Design of an elliptically bent refocus mirror for the MERLIN beamline at the advanced light source," NIM A, 582(1), 135-137 (2007).

[3] Howells, M. R., Cambie, D., Duarte, R. M., Irick, S., MacDowell, A. A., Padmore, H. A., Renner, T. R. *et al.*, "Theory and practice of elliptically bent x-ray mirrors," Optical Engineering, 39(10), 2748-2762 (2000).

[4] Yuan, S., Goldberg, K. A., Yashchuk, V. V., Celestre, R., McKinney, W. R., Morrison, G., Macdougall, J. *et al.*, "Cross-check of ex-situ and in-situ metrology of a bendable temperature stabilized KB mirror," NIM A, 635(1, Supplement 1), S58-S63 (2011).
[5] Yuan, S., Yashchuk, V. V., Goldberg, K. A., Celestre, R., McKinney, W. R., Morrison, G. Y., Warwick, T. *et al.*, "Development of in situ, at-wavelength metrology for soft X-ray nano-focusing," NIM A, 649(1), 160-162 (2011).
[6] Yuan, S., Goldberg, K. A., Yashchuk, V. V., Celestre, R., Mochi, I., Macdougall, J., Morrison, G. Y. *et al.*, "At-wavelength optical metrology development at the ALS," Proc. SPIE 7801, 78010D-13 (2010).
[7] Yuan, S., Church, M., Yashchuk, V., Goldberg, K. A., Celestre, R., McKinney, W., Kirschman, J. *et al.*, "Elliptically Bent X-Ray Mirrors with Active Temperature Stabilization," X-Ray Optics and Instrumentation, Vol. 2010, Article ID 784732 (2010).
[8] Rah, S., and Howells, M. R., "Representation of conic surfaces and conic cylinders with vertex coordinates system for design and assessment of grazing incidence optics," LSBL-382, Lawrence Berkeley National Laboratory (1997).
[9] Ugural, A. C., and Fenster, S. K., [Advanced Strength and Applied Elasticity], Prentice Hall, Englewood Cliffs, NJ (1995).
[10] Marcus, M. A., MacDowell, A. A., Celestre, R., Manceau, A., Miller, T., Padmore, H. A., and Sublett, R. E., "Beamline 10.3.2 at ALS: a hard X-ray microprobe for environmental and materials sciences," J. Synchrotron Rad., 11, 239-247 (2004).
[11] Howells, M. R., "Partial correction of spherical aberration in mirrors (gravitational or intrinsic) by means of deliberate defocus," LSBL-360, Lawrence Berkeley National Laboratory (1997).
[12] McKinney, W. R., Irick, S. C., Kirschman, J. L., MacDowell, A. A., Warwick, T., and Yashchuk, V. V., "New procedures for the adjustment of elliptically bent mirrors with the long trace profiler," Proc. SPIE 6704, 67040G-12 (2007).
[13] McKinney, W. R., Kirschman, J. L., MacDowell, A. A., Warwick, T., and Yashchuk, V. V., "Optimal tuning and calibration of bendable mirrors with slope-measuring profilers," Optical Engineering, 48(8), 083601-8 (2009).
[14] Yashchuk, V. V., "Positioning errors of pencil-beam interferometers for long trace profilers," Proc. SPIE 6317, 63170A-12 (2006).
[15] Plackett, R. L., [Principles of Regression Analysis], Clarendon Press, Oxford (1960).
[16] Hudson, D., [Lectures on Elementary Statistics and Probability], CERN, Geneva (1963).
[17] Neter, J., and Wasserman, W., [Applied Linear Statictical Models], Inwin-Dorsey International, London (1974).
[18] Kendall, M., and Stuart, A., [The Advanced Theory of Statistics], Oxford University Press, New York (1979).
[19] Lawrence, G. N., and Moore, K. E., "Optical design and optimization with physical optics," Proc. SPIE 1354, 15-22 (1991).
[20] Kalman, D., "General Equation of an Ellipse," http://www.maa.org/joma/Volume8/Kalman/General.html, J. Online Math. and its Appl., 2008.
[21] Alcock, S. G., Ludbrook, G. D., Owen, T., and Dockree, R., "Using the power spectral density method to characterise the surface topography of optical surfaces," 7801, 780108 (2010).
[22] Rommeveaux, A., Assoufid, L., Ohashi, H., Mimura, H., Yamauchi, K., Qian, J., Ishikawa, T. *et al.*, "Second metrology round-robin of APS, ESRF and SPring-8 laboratories of elliptical and spherical hard-x-ray mirrors," Proc. SPIE 6704, 67040B-12 (2007).
[23] Zhang, L., Baker, R., Barrett, R., Cloetens, P., and Dabin, Y., "Mirror profile optimization for nano-focusing KB mirror," AIP Conference Proceedings, 1234(1), 801-804 (2010).